JOURNAL OF AIRCRAFT
Vol. 36, No. 6, November–December 1999

Comparison of Multidisciplinary Design Optimization Codes for Conceptual and Preliminary Wing Design

Richard Butler*
University of Bath, Bath, England BA2 7AY, United Kingdom
Erik Hansson†
Saab AB, 581 88 Linköping, Sweden
Mark Lillico‡
University of Bath, Bath, England BA2 7AY, United Kingdom
and
Frank Van Dalen§
Delft University of Technology, 2629 HS Delft, The Netherlands

The results produced by two multidisciplinary design optimization programs for the analysis and optimum design of a benchmark regional aircraft wing are compared. One of the programs uses a simple beam model and is suitable for conceptual design whereas the other uses a three-dimensional finite element model and is suitable for preliminary design. Results for stress, displacement, vibration, and flutter analyses of the initial design configuration show good agreement, as do those for optimization with stress and flutter constraints. However, optimization for a set of limiting wing twist displacements caused by aileron loading shows a 20% difference in design variable mass between the two models, with the preliminary design model producing the lower mass design. This can be explained by the ability of the detailed finite element model to allow for chordwise variation in skin thickness and chordwise bending effects. Furthermore, the deflection constraints used are obtained from a similar finite element model that has been optimized for aileron efficiency and therefore present particular problems when using the beam model, which does not allow for such chordwise variation.

I. Introduction

THE initial stage of wing design normally consists of an estimate of wing mass using a statistical data base. During the initial structural sizing stage that follows this stage, design constraints relating to the interaction of wing structure and aerodynamics are frequently neglected, i.e., aeroelastic effects such as flutter and aileron roll efficiency. As a consequence, these effects often cause problems later in the design cycle and require expensive design modifications. A variety of optimization programs that include aeroelastic constraints have been developed for structural sizing. Some of these involve fairly simple models that are suitable for conceptual structural design, e.g., Refs. 1–3, whereas others use fully three-dimensional finite element (FE) models that may be applied at the preliminary/detailed design stage, e.g., Refs. 4–7.

The purpose of this paper is to compare the results produced by two multidisciplinary optimization codes for the design of a 70-seat regional aircraft wing. One of the codes[3] is suitable for use at the conceptual design stage whereas the other[4,7] may also be used during preliminary design. This paper will indicate the suitability and restrictions of the two approaches during the design cycle. The results, along with those produced by other codes, are currently being obtained by a GARTEUR (Group for Aeronautical Research and Technology in Europe) Action Group on Multidisciplinary Wing Optimization. The same practical benchmark wing problem as is extensively covered by the GARTEUR work is used here.

Received 15 July 1998; presented as Paper 98-4857 at the AIAA/USAF/NASA/ISSMO 7th Symposium on Multidisciplinary Analysis and Optimization, St. Louis, MO, 2–4 September 1998; revision received 10 March 1999; accepted for publication 20 May 1999.

*Senior Lecturer in Aircraft Structures, Department of Mechanical Engineering.
†Research Engineer, Future Products and Technology.
‡Research Assistant, Department of Mechanical Engineering.
§Research Engineer, Department of Aerospace Engineering, Kluyverweg 1.

II. Example Problem

The benchmark aircraft[8] was designed specifically for the GARTEUR Action Group on Multidisciplinary Wing Optimization. The research goal of this group is to integrate structural optimization techniques and aeroelastic requirements in the conceptual and preliminary design stages of an aircraft.

The specifications for the aircraft were intended to represent a realistic and up-to-date design problem, matching the GARTEUR partners' design backgrounds. Hence, the choice of a 70-seat regional jet that cruises at $M_C = 0.70$. Propulsion is by two ultra-high bypass turbofans. The wing area was 93 m^2 and the takeoff weight was 35,847 kg. It is worth noting that one of the aims of the GARTEUR Action Group was to study the effect of wing aspect ratio on range and direct operating cost. However, the results of this study are not covered in this paper and the example problem used for the comparison of the two codes is based on the $AR = 15.5$ GARTEUR wing (see Fig. 1) because this shows the most interesting aeroelastic effects.

A substantial amount of data were generated using the Aircraft Design and Analysis System (ADAS)[9] to complete the benchmark. For static loads as well as eigenmode analysis, a realistic mass distribution is required. The weight breakdown for the aircraft, produced according to Ref. 10, includes a number of empty weight contributions as well as payload, cargo, and inboard and outboard fuel tank contents. Each of these contributions is mapped to a number of model nodes, and the distribution of the total mass contribution among these nodes is weighted in X, Y, and Z directions to obtain the correct center of gravity location. For the purpose of eigenmode analysis, the wing is assumed to be fully fixed at the position of the aircraft centerline; hence, the aircraft is not modeled in its free-free state, and only symmetrical wing modes are accounted for during flutter analysis.

The flight envelopes for maneuver and gust loading conditions were calculated for maximum zero fuel weight at an altitude of 6100 m. Because the aircraft is critical in gust loading conditions, the four cases that are used in the static strength optimization of the

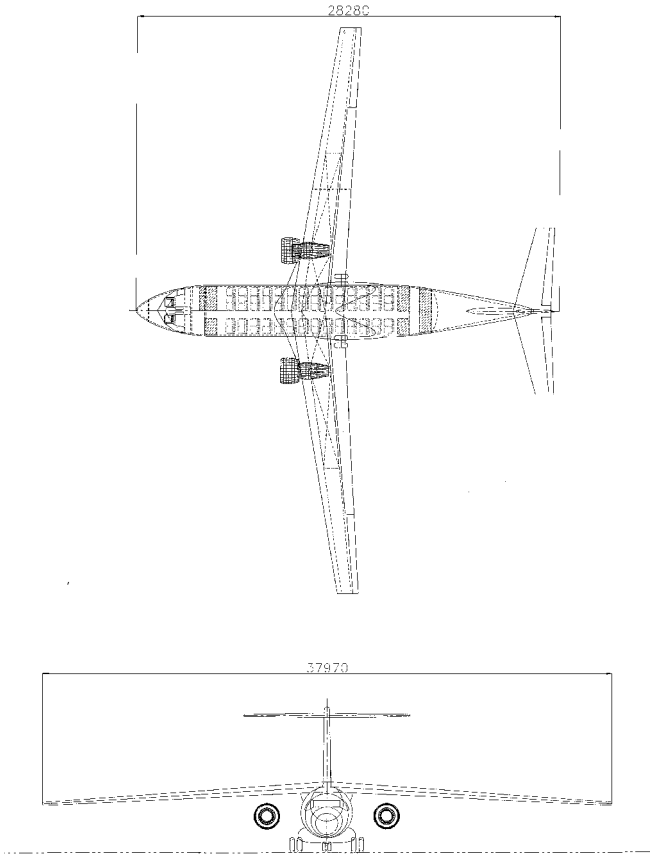

Fig. 1 The GARTEUR benchmark aircraft ($AR = 15.5$), dimensions in millimeters.

model are the four extreme gust conditions at aircraft speeds of 370 and 465 km/h (equivalent air speed) and accelerations of +2.91 and $-0.91g$. For each of these conditions, the lift distribution along the wing is calculated using Diederich's method described in Ref. 11. A fifth aileron deflection load case is also applied to provide the loading for a set of wing twist displacement constraints to represent an aileron roll efficiency constraint for the wing. In this case the wing is also assumed to be fully fixed at the position of the aircraft centerline.

The material selected for the lower skin is Al 2024-T3 alloy and Al 7075-T6 for all other structural elements. In both models presented, the stringers have been smeared onto the skins and are accounted for by adjusting the skin material properties. The allowable stresses for standard structural components of light alloy of given structural dimensions are found using Ref. 9. These stresses are based on a number of criteria including material strength, skin buckling, flexural buckling, and residual strength of a cracked panel. This means that during structural optimization, the allowables should be updated as they respond to changes in thickness. To bypass such a complication, the allowable stresses that are finally used in the optimization are based on a structural thickness distribution that is taken from an initial sizing of the wing using the fully stressed design principle on a single stress analysis result. The allowables therefore depend on the load intensity in the structure, which varies along the wing span. The entire data processing sequence described was fully automated and thus generating the models and data was a trivial task.

Optimization that seeks to minimize the structural weight of the complete wing has been carried out for the following four constraint cases.

1) Case S (Stress constraints): Here the preceding stress constraints are applied, along with minimum thickness constraints.

2) Case S + F (Stress and Flutter constraints): This is the same as case S but includes a minimum flutter speed constraint of 290 m/s at 4572 m.

3) Case S + D (Stress and Displacement constraints): This is the same as case S but includes the twist displacement constraints at a number of stations along the wing for the aileron load case.

4) Case S + D + F (Stress, Displacement, and Flutter constraints): This is the same as case S + D but includes a minimum flutter speed constraint of 290 m/s at 4572 m.

III. Conceptual Design Model

Conceptual design has been carried out using the program CALFUNOPT,[3] which models the wing as a series of box-beam elements and uses the dynamic stiffness method (DSM) to find normal modes before applying generalized coordinates and strip theory to calculate the flutter speed. The DSM involves the exact solution of the equations of motion for each element and, hence, more elements are not required to improve accuracy, provided the number of constant-section elements used produces an adequate representation of the tapered wing. This approach differs from traditional FE methods that approximate displacements with shape functions and, therefore, require more elements to improve accuracy.

For the CALFUNOPT results presented in Sec. V, the wing has been modeled as an 11-element cantilever fixed at the aircraft centerline, with element 11 representing the wing within the fuselage. Quadratic-linking equations are used to represent the spanwise thickness distributions in the front spar, rear spar, upper skin, and lower skin of elements 1–10. Thus only three design variables are needed to give the thickness distribution of each structural component for these elements, giving a total of 12 design variables for the problem. (These design variables are the thicknesses of each of the four components in elements 1, 6, and 10.) The wing box is assumed to be rectangular with constant chordwise skin thickness and the upper skin, lower skin, and spars can each have different material properties. Nonstructural mass is represented by lumping mass along the front and rear spars. The booms (or spar caps) that are not design variables are smeared onto the skin when calculating the bending rigidity of the wing but are ignored during torsional rigidity calculations.

For constraint case S + D + F, there is one flutter constraint, 10 displacement constraints (which limit the difference in vertical displacement between the front and rear spars at the root of each element for the aileron deflection loading), and 60 sets of stress constraints, i.e., six sets for each of the 10 wing elements to represent different material strength of upper and lower skins, front and rear spars, and upper and lower booms. Only the most severe gust load case is considered, but because this case is critical, comparisons with the code described next are valid. For this load case, the inboard value of shear force, bending moment, and torque for each element is calculated assuming a constant spanwise acceleration of $2.91g$ at 165 m/s and 4572 m, a constant spanwise C_{mo} of -0.05, and the same C_L distribution used to calculate the preliminary design model loads.

IV. Preliminary Design Model

Several steps were taken to develop the general arrangement drawing shown in Fig. 1 into a three-dimensional FE model with appropriate mass and stiffness distribution. As a first step, the general arrangement was read into ADAS and a three-dimensional surface model of one-half of the aircraft was generated (see Fig. 2) because all analysis cases can be represented by one-half aircraft model. The surface model was read into an FE preprocessor, in IGES (Initial Graphics Exchange Specification) format, to create the FE model of the aircraft in NASTRAN[12] Bulk Data Deck format. This model was then read back into ADAS for further processing; see Fig. 3. The engine and the pylon are represented by beam elements and the wing root rib is attached to the fuselage centerline by means of beam elements. The spar and rib webs are represented by membrane elements, and the skins are represented by membrane elements with modified orthotropic material properties to account for the elastic properties of the stringers. It should be noted that, for the FE model, using membrane rather than shear elements for the spars has the tendency to make the wing model slightly overstiff. Rod elements run along the tops and bottoms of the spars and around the two main ribs.

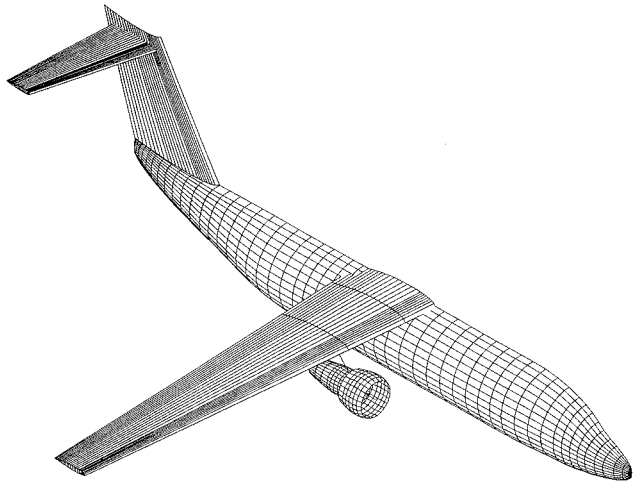

Fig. 2 Surface model of benchmark aircraft.

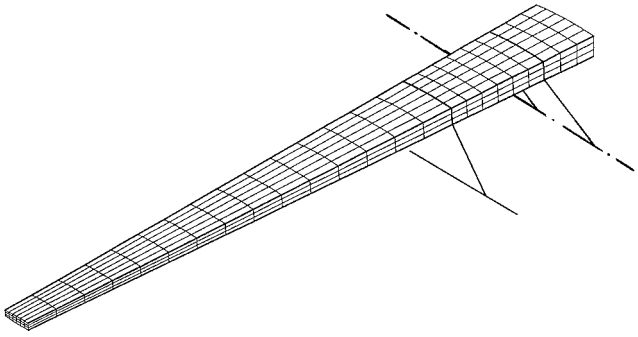

Fig. 3 FE model of wing.

The wing lift forces are applied to the upper spar caps of the front and rear spars and the inertia loads balancing these aerodynamic forces are calculated using the linear and angular acceleration of the whole aircraft and are applied to all nodal masses of the model. A special interface was written to merge the geometrical FE data with the mass, stiffness, and loads data generated in ADAS in an update of the Bulk Data Deck. The model could then be analysed in NASTRAN.

The preliminary design optimization presented in the following section has been performed with the program OPTSYS,[4,13] which can optimize a number of standard FE models. In this case, a NASTRAN model is used. For the flutter calculations, an in-house Doublet Lattice code has been used and, for the linking between FE elements and design variables, the wing has been divided into eight constant thickness bays in the spanwise direction. For each of these bays, there are three (chordwise) design variables for each skin and one design variable for each spar web. Hence, each skin variable is three elements long and two elements wide (see Fig. 3). This, along with some additional design variables for ribs, gives a total of 75 design variables for the problem.

V. Discussion of Results

First, results for the analysis of the initial (unoptimized) design are presented. These are followed by results for the various optimization cases described in Sec. II. It should be noted that, in each optimization case, the optimum designs produced by both programs are feasible, i.e., have satisfied constraints.

The difference in initial masses (see Table 1) is because the initial design variables have been modified to satisfy the minimum thickness constraints in the CALFUNOPT case. Figure 4 shows that, as expected, the CALFUNOPT beam model is slightly stiffer

Table 1 Comparison of conceptual (CALFUNOPT) and preliminary (OPTSYS) design results

Descriptor		CALFUNOPT	OPTSYS
Initial design natural frequencies, Hz	1 VB	0.94	1.04
	1 HB	2.11	2.16
	2 VB	3.82	3.52
	EY	——	5.35
	2 VB + EP	6.09	5.84
Flutter speed, m/s TAS at 15,000 ft	Initial	154	164
	S	224	177
	S + F	290	>306
	S + D	188	177
	S + D + F	293	>294
Design variable mass, kg	Initial	1282	1232
	S	1180	1189
	S + F	1248	1308
	S + D	1917	1586
	S + D + F	1932	1602

Note: For the natural frequency results, VB, HB, EY, and EP refer to vertical and horizontal bending, and engine yawing and pitching modes of vibration, respectively. S, D, and F refer to stress, displacement, and flutter constrained optimization, respectively.

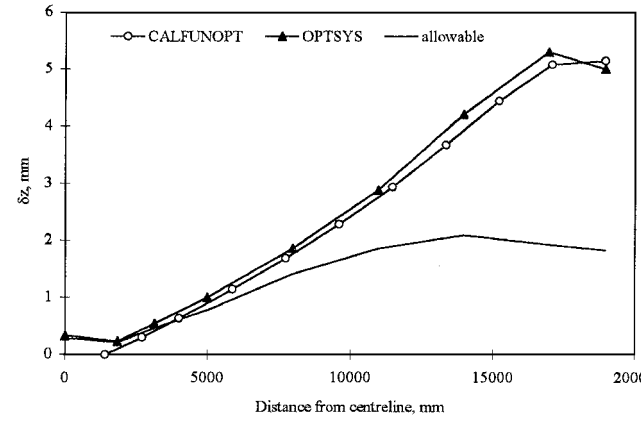

Fig. 4 Spanwise variation of twist for initial design with aileron loading applied. (The δz is the difference in front and rear spar vertical displacement, positive if rear spar deflection is greater.)

in twist than the OPTSYS FE model, and that both sets of displacements are significantly greater than the allowable values for the aileron loading. The spanwise variation of the most significant stresses for the critical gust case produced by both programs is given in Fig. 5. The more detailed stress distribution produced by the FE program is evident, although it can be seen that the general trends are similar. The beam model calculates the stress in the middle of each of the 10 elements whereas, for the FE model, stress is calculated for each of the three spanwise elements in each of the eight bays. For the latter, the maximum chordwise value of skin stress is plotted and the skin and spar thicknesses in each bay are constant. Hence, there is a discontinuity in stress distribution between bays because of the change in thickness for the OPTSYS result. The natural frequencies, mode shapes, and flutter speeds for the initial design (Table 1) show reasonable agreement between the two programs. In both cases, flutter is driven by the first horizontal bending mode, which, because of the inertia caused by the engine, produces a small amount of wing twist and very little aerodynamic damping.

For each program, Table 1 compares the optimum values of both design variable mass and flutter speed for optimization with stress constraints (case S); stress and flutter constraints (case S + F); stress and displacement constraints (case S + D); and stress, displacement, and flutter constraints (case S + D + F). The optimum values of the design variables for all cases, with the exception of case S + F, are given in Figs. 6 and 7. It should be noted that the thickness plots given

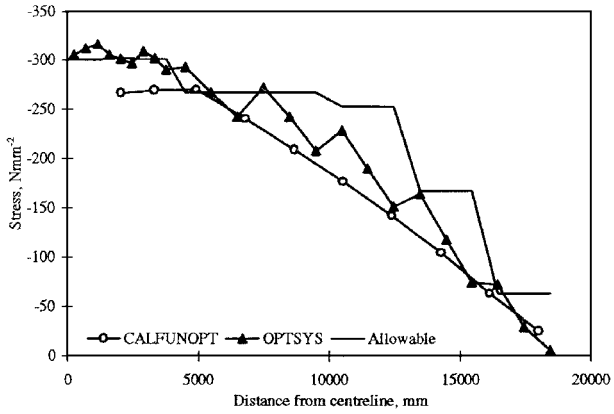

a) Upper skin compression

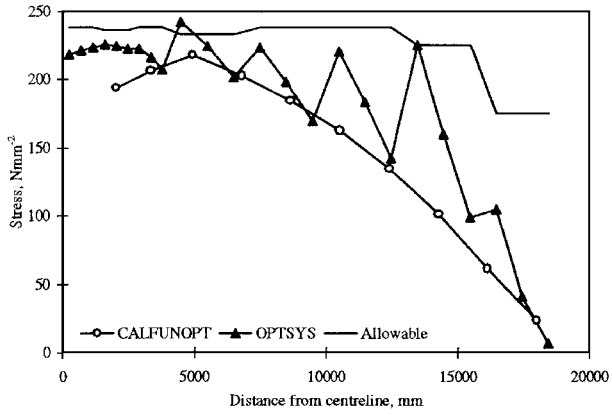

b) Lower skin tension

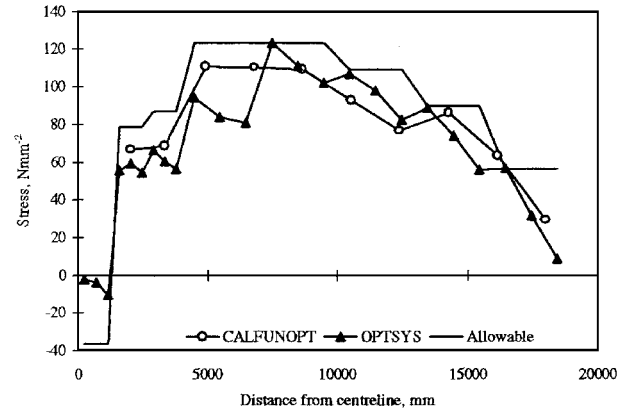

c) Front spar shear

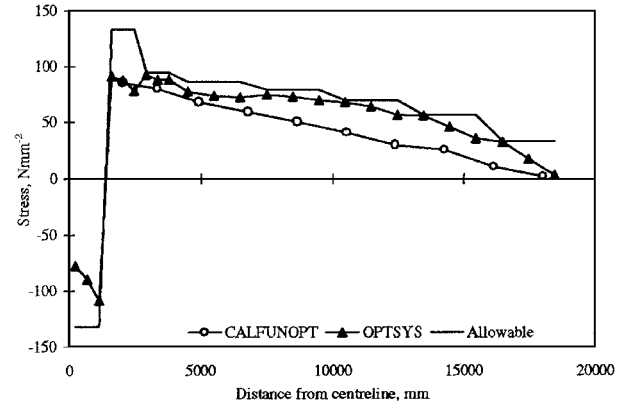

d) Rear spar shear

Fig. 5 Spanwise variation in initial design stress for critical gust case.

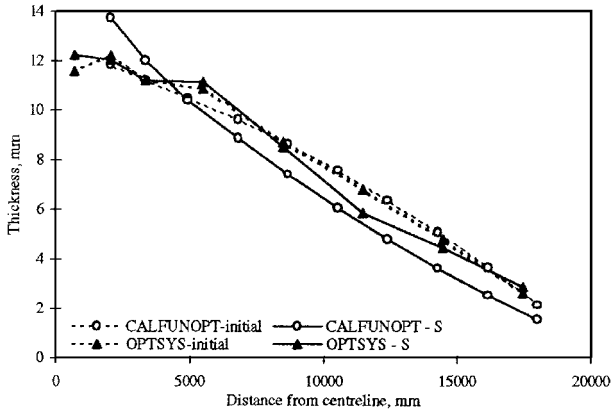

a) Upper skin

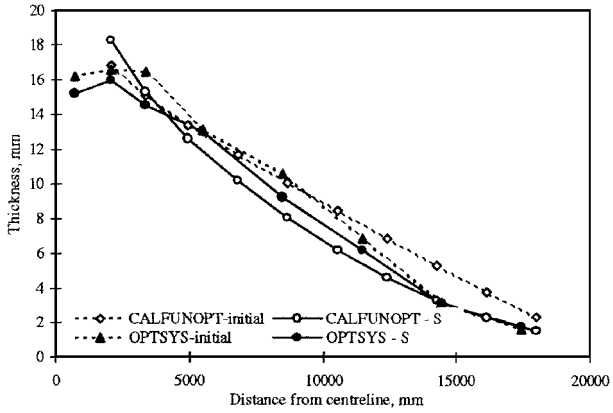

b) Lower skin

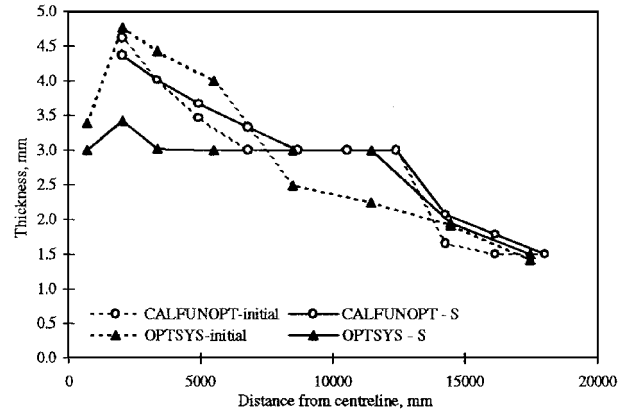

c) Front spar

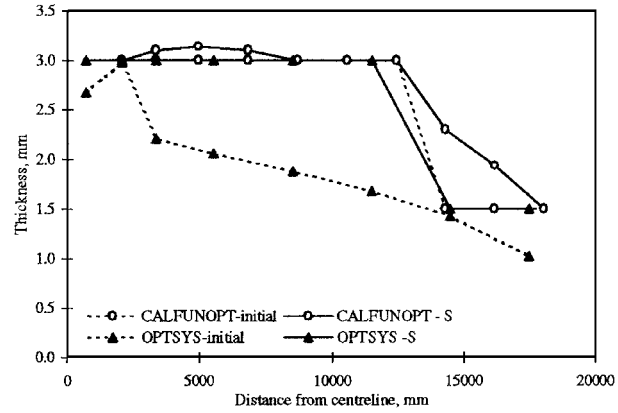

d) Rear spar

Fig. 6 Initial thicknesses and optimum design thicknesses for stress constraints (case S).

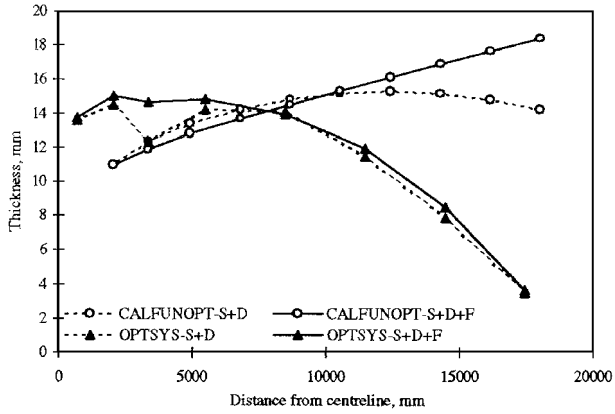

a) Upper skin

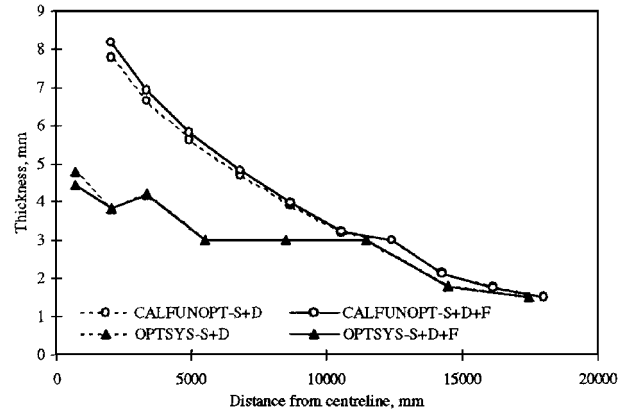

c) Front spar

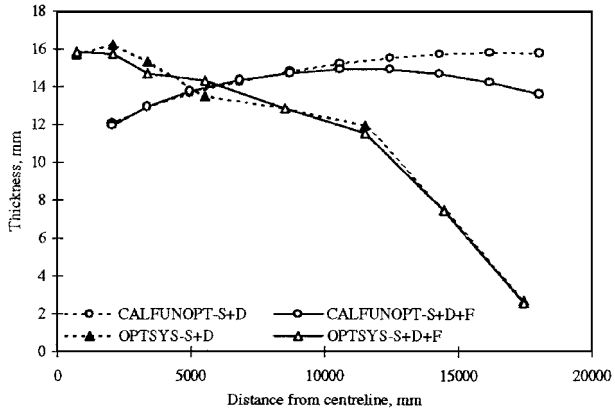

b) Lower skin

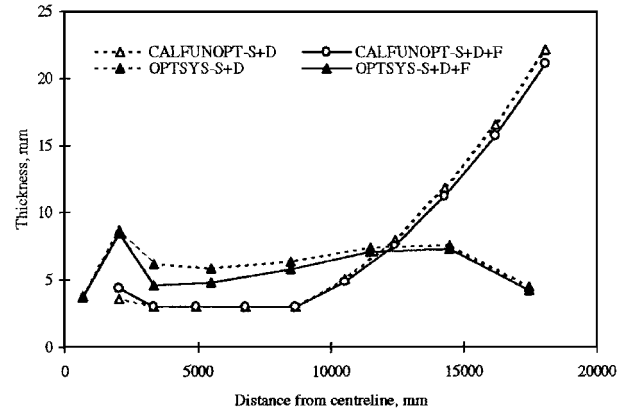

d) Rear spar

Fig. 7 Optimum design thicknesses for stress and displacement constraints (case S + D) and stress, displacement, and flutter constraints (case S + D + F).

in these figures do not show the step changes that occur between each of the 8 spanwise bays and 10 spanwise elements used in OPTSYS and CALFUNOPT, respectively. It should also be noted that the OPTSYS skin thicknesses shown in these figures are the averages of the three chordwise design variables described in Sec. IV. Figure 8 shows these chordwise variables, before averaging.

Case S

The optimum design variable masses for this case are very similar, and Fig. 6 shows a small deviation between the two optimum designs. However, Table 1 shows a marked difference in flutter speeds for the two designs. This may be explained by the thicker upper skin produced by OPTSYS toward the wing tip. In this region, a higher elastic axis tends to produce aerodynamic forcing that counteracts the aerodynamic forcing resulting from the pitching inertia of the engine, thereby delaying flutter onset.

Case S + F

The CALFUNOPT optimum is 5% lighter than the corresponding OPTSYS design in this case. This is probably because the aerodynamic strip theory used by the former will tend to overestimate flutter speed in the transonic range.

Cases S + D and S + D + F

Figure 7 shows that, whereas the effect of adding the flutter constraint to both programs is small, the results produced by the two programs differ significantly. The CALFUNOPT designs are about 20% heavier than the OPTSYS designs (see Table 1). This can be explained by the ability of the detailed FE model to satisfy the deflection constraint by producing a large variation in chordwise skin thickness (see Figs. 8b and 8c). The aileron loading is concentrated around the rear spar and therefore OPTSYS moves skin material toward the rear spar where the effect of the constraint dominates, i.e., at the midspan. This moves the torsional center of the wing box toward the rear spar and reduces the effective torque on the wing. The CALFUNOPT beam model represents the aileron load case as a spanwise bending moment and torque distribution, where the torque is calculated about the torsional center of the box, which can vary during optimization. It satisfies the deflection constraint by increasing the bending and torsional rigidity of each box element and by thickening the rear spar, which reduces the torque loading produced by the aileron. Here, the increase in bending rigidity reduces the additional nosedown twist caused by the upbending of the slightly (7.9 deg) sweptback wing. The detailed OPTSYS FE model, which allows for chordwise bending, can counteract this effect by using a small amount of material around the leading edge (see Figs. 7c and 8b and 8c).

It should also be noted that the deflection constraints were obtained from an FE model, similar to the OPTSYS model, but optimized for aileron roll efficiency. It is, therefore, more likely that OPTSYS will be able to satisfy the deflection constraints more efficiently than the beam model of CALFUNOPT.

The addition of the flutter constraint produces designs that are only about 20 kg heavier using both programs, and only small adjustments to the case S + D designs are required (see Fig. 7). The effect of these adjustments is to move the torsional axis upward toward the wing tip by thickening the upper skin and, in the case of the CALFUNOPT design, reducing the lower skin thickness. As explained earlier, this causes the outboard section of the wing to counteract the twist caused by the inertia of the engine in the first horizontal bending mode, thereby delaying flutter onset.

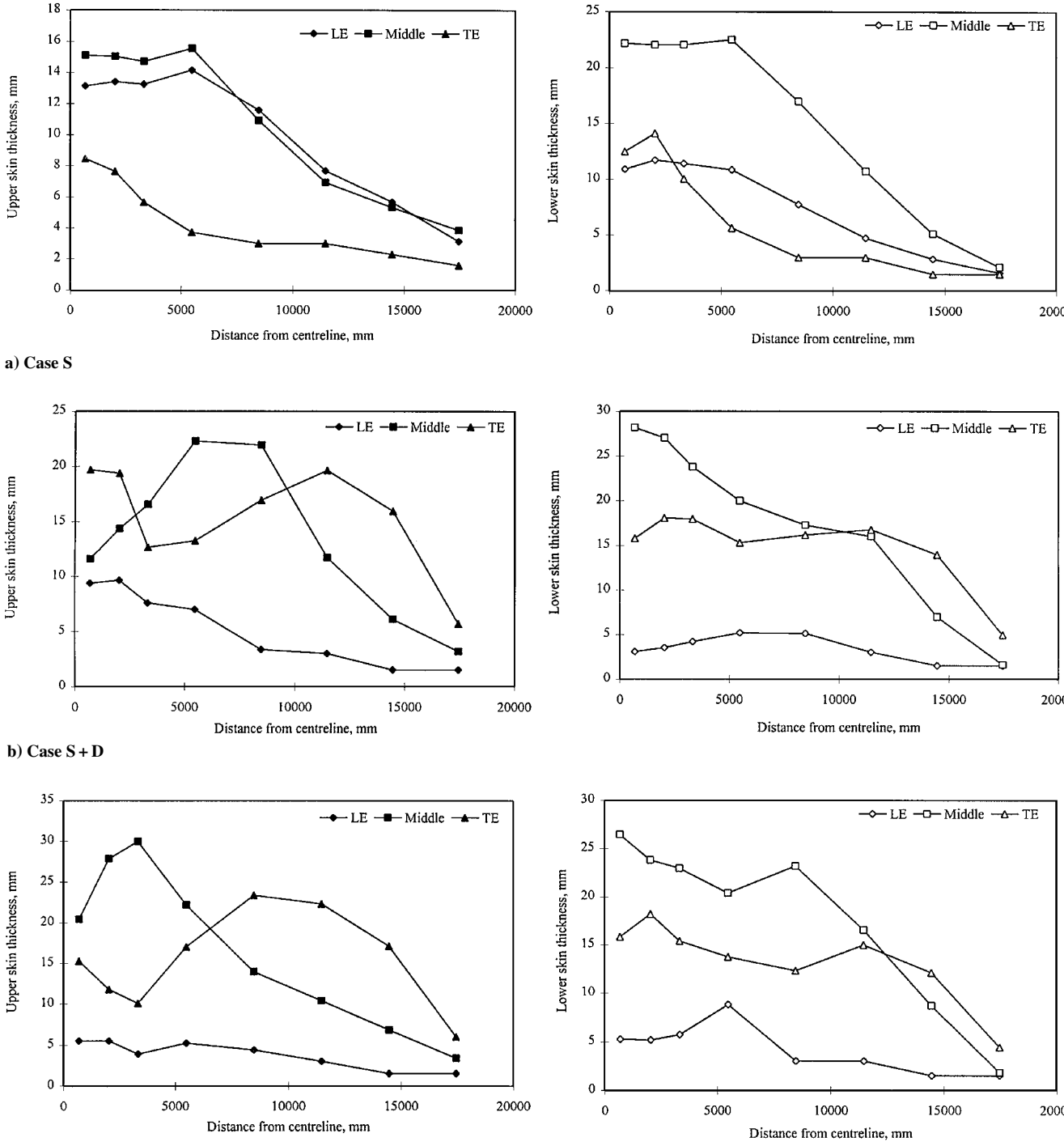

Fig. 8 Chordwise and spanwise variation of OPTSYS optimum skin thicknesses: LE = leading edge and TE = trailing edge.

VI. Conclusions

For analysis of the initial design, the displacement, stress, vibration, and flutter results produced by the two models are similar. The main differences in the models would appear to be the ability to formulate a more detailed optimum design in the preliminary design model but not in the conceptual model. This presents particular advantages for optimization with the deflection constraints when aileron loading is applied. However, it should be stated that the deflection constraints used are based on an aileron efficiency of 53%. This is severe for a wing of this aspect ratio and, therefore, presents particular problems when using the beam model, which does not, at present, allow for a variation in chordwise skin thickness. However, it is worth noting that it would be difficult to manufacture a wing with the large chordwise variation in thickness produced by the preliminary design model. For a more realistic aileron efficiency, it is expected that the differences between the two programs would be much smaller.

The conceptual design model uses a dedicated pre- and postprocessor whereas the preliminary design model can use any standard FE pre- and postprocessor. As expected, the conceptual design model is simpler to construct and interpret than the preliminary design model because of both a smaller structural model and fewer design variables. Furthermore, the loading for stress constraint calculations is calculated within the conceptual model, but is derived externally for the preliminary design model. Hence, one might expect the conceptual (beam) model to be used after the external geometry and initial mass distribution of the aircraft has been established. The resulting structural/aeroelastic design could then be transferred

to the preliminary (FE) design model for further refinement. Such a process would improve the fidelity of the initial FE model, thereby saving modeling effort.

Acknowledgments

The authors are grateful to GARTEUR for permission to give the necessary information about the benchmark problem. They are also grateful to G. Schneider of Daimler-Benz Aerospace for providing the aileron deflection loading and the associated wing twist constraints, and to M. A. Spink of the University of Bath for his help in formulating the CALFUNOPT deflection constraints.

References

[1]Wilkinson, K., Markowitz, J., Lerner, E., George, D., and Batill, S. M., "Fastop: A Flutter and Strength Optimization Program for Lifting-Surface Structures," *Journal of Aircraft*, Vol. 14, No. 6, 1977, pp. 581–587.

[2]Austin, F., Hadock, R., Hutchings, D., Sharp, D., Tang, S., and Waters, S., "Aeroelastic Tailoring of Advanced Composite Lifting Surfaces in Preliminary Design," *Proceedings of the AIAA/ASME/SAE 17th Structures, Structural Dynamics, and Materials Conference*, AIAA, New York, 1976, pp. 69–79.

[3]Lillico, M., Butler, R., Guo, S., and Banerjee, J. R., "Aeroelastic Optimization of Composite Wings Using the Dynamic Stiffness Method," *Aeronautical Journal*, Vol. 101, No. 1002, 1997, pp. 77–86.

[4]Bråmå, T., "Weight Optimization of Aircraft Structures," *Computer Aided Optimal Design: Structural and Mechanical Systems*, edited by Mota Soares, Springer–Verlag, Berlin, 1987, pp. 971–985.

[5]Neill, D. J., Johnson, E. H., and Canfield, R., "ASTROS—A Multidisciplinary Automated Structural Design Tool," *Journal of Aircraft*, Vol. 27, No. 12, 1990, pp. 1021–1027.

[6]Bartholomew, P., and Wellen, H. K., "Computer—Aided Optimization of Aircraft Structures," *Journal of Aircraft*, Vol. 27, No. 12, 1990, pp. 1079–1086.

[7]Bråmå, T., and Rosengren, R., "Applications of Structural Optimization Software in the Design Process," *Journal of Aircraft*, Vol. 27, No. 12, 1990, pp. 1057–1060.

[8]Fransen, S. H. J. A., "Conceptual Design of a 70 Passenger Airliner Propelled by Fuel-Efficient Turbofan Engines," Memorandum M-725, Faculty of Aerospace Engineering, Delft Univ., Delft, The Netherlands, March 1996.

[9]Van Dalen, F., and Rothwell, A., "ADAS Structures Module: User's Manual," Memorandum M-709, Faculty of Aerospace Engineering, Delft Univ., Delft, The Netherlands, May 1995.

[10]Torenbeek, E., "Synthesis of Subsonic Airplane Design," Delft Univ. Press, Nijhoff, The Netherlands, 1988.

[11]Diederich, F. W., "A Simple Approximate Method for Calculating Spanwise Lift Distributions and Aerodynamic Influence Coefficients at Subsonic Speeds," NACA TN-2751, 1952.

[12]*NASTRAN User's Manual*, Vol. 1, NASA SP-222(08), June 1996.

[13]Bråmå, T., "The Structural Optimization System OPTSYS," *International Series of Numerical Mathematics*, Birkhäuser Verlag, Berlin, 1993, pp. 187–206.